THE PROTEIN SOCIETY

Penetration into membrane of amino-terminal region of SecA when associated with SecYEG in active complexes

Bahar T. Findik,[1] Virginia F. Smith,[2] and Linda L. Randall[1]*

[1]Department of Biochemistry, 117 Schweitzer Hall, University of Missouri, Columbia, Missouri 65211
[2]Chemistry Department, U.S. Naval Academy, Annapolis, Maryland 21402

Received 3 October 2017; Accepted 14 December 2017
DOI: 10.1002/pro.3362
Published online 16 December 2017 proteinscience.org

Abstract: The general secretory (Sec) system of *Escherichia coli* translocates both periplasmic and outer membrane proteins through the cytoplasmic membrane. The pathway through the membrane is provided by a highly conserved translocon, which in *E. coli* comprises two heterotrimeric integral membrane complexes, SecY, SecE, and SecG (SecYEG), and SecD, SecF, and YajC (SecDF/YajC). SecA is an associated ATPase that is essential to the function of the Sec system. SecA plays two roles, it targets precursors to the translocon with the help of SecB and it provides energy via hydrolysis of ATP. SecA exists both free in the cytoplasm and integrally membrane associated. Here we describe details of association of the amino-terminal region of SecA with membrane. We use site-directed spin labelling and electron paramagnetic resonance spectroscopy to show that when SecA is co-assembled into lipids with SecYEG to yield highly active translocons, the N-terminal region of SecA penetrates the membrane and lies at the interface between the polar and the hydrophobic regions, parallel to the plane of the membrane at a depth of approximately 5 Å. When SecA is bound to SecYEG, preassembled into proteoliposomes, or nonspecifically bound to lipids in the absence of SecYEG, the N-terminal region penetrates more deeply (8 Å). Implications of partitioning of the SecA N-terminal region into lipids on the complex between SecB carrying a precursor and SecA are discussed.

Keywords: SecA; EPR; power saturation; SecYEG proteoliposomes; protein–lipid interactions; depth in bilayer; protein export

Introduction

The general secretory (Sec) system of *Escherichia coli* translocates both periplasmic and outer membrane proteins through the cytoplasmic membrane. The pathway through the membrane is provided by a highly conserved translocon, which in *E. coli* comprises two heterotrimeric membrane complexes, SecY, SecE and SecG (SecYEG), and SecD, SecF and YajC (SecDF/YajC).[1] Exported proteins must pass through the translocon before they acquire stably-folded tertiary structure.[2] The precursor polypeptides are maintained in an unfolded state by association with cytosolic factors: SecB, a chaperone, and SecA, an ATPase. SecA, both with and without SecB, forms complexes with precursor polypeptides and delivers them to the translocon through an affinity for SecY. *In vivo* SecA is equally distributed between a soluble state in the cytoplasm and associated with the cytoplasmic membrane.[3] A fraction of the membrane-associated population is integral to the membrane; it cannot be removed by treatments

Additional Supporting Information may be found in the online version of this article.

Grant sponsor: National Institute of General Medical Sciences; Grant number: 29798; Grant sponsor: Hugo Wurdack Trust at University of Missouri.

*Correspondence to: Linda L. Randall; Department of Biochemistry, 117 Schweitzer Hall, University of Missouri, Columbia, MO 65211. E-mail: craneje@missouri.edu

used to define proteins as peripheral membrane proteins.[4–6] SecA is expected to be membrane associated since it binds SecY with high affinity.[7–9] However, even in the absence of SecYEG, SecA binds to liposomes that contain anionic lipids. This binding is nonspecific and mediated through electrostatic and hydrophobic interactions.[10] Two lipid-binding regions have been identified: the extreme carboxyl-terminal 70 aminoacyl residues of SecA, which are responsible for the electrostatic interactions,[11] and the amino-terminal region, which is responsible for the hydrophobic binding.[10] A bioinformatics approach has identified eight additional regions distributed throughout the protein that are possible lipid-binding sequences.[12]

There is experimental evidence from many laboratories that SecA inserts into phospholipids.[13–19] Here we use site-directed spin labelling and electron paramagnetic resonance spectroscopy to measure depth in the lipid bilayer. We show that both in the absence of SecYEG and when productively associated with the translocon, the N-terminal twenty aminoacyl residues of SecA penetrate the membrane to lie at the interface between the polar heads and the hydrophobic interior, parallel to the plane of the membrane.

Results

In our laboratory, we use two reconstitution systems to study protein export. One is the conventional system in which the integral membrane complex SecYEG is assembled with *E. coli* lipids (termed proteoliposomes SecYEG, abbreviated PLYEG) and in the other SecYEG is assembled into liposomes in the presence of SecA (abbreviated PLYEG•A). The co-reconstitution of SecA with SecYEG results in a six-fold increase in the number of active translocons as compared to PLYEG to which SecA is added after reconstitution.[20] The co-reconstitution system presents a good model for the *E. coli* cytoplasmic membrane because the fraction of the total SecYEG present that is active is the same for PLYEG•A and for isolated native inner membrane vesicles.[20] We have used electron paramagnetic resonance (EPR) spectroscopy coupled with site-directed spin labeling to examine the immersion depth of the N-terminal region of SecA when it is bound to SecYEG in highly active complexes created by co-assembly into proteoliposomes PLYEG•A, as well when SecA is added after reconstitution of SecYEG into PLYEG, and when SecA is added to liposomes that do not contain SecYEG.

The basis for determination of depth within a membrane using EPR spectroscopy is the phenomenon of power saturation. The intensity of an EPR signal reflects the difference in spin populations between the upper and lower energy states, which is proportional to the extent of microwave energy absorbed. The difference in the populations decreases as energy is absorbed. The population is restored to thermal equilibrium by dissipation of the excess energy through transfer to the surroundings (spin–lattice relaxation) to allow further absorption of energy. The time taken for the spin system to relax to equilibrium determines the amount of incident microwave power required to reach saturation of the signal. A shift of saturation to higher power can be achieved experimentally by addition to the solvent of paramagnetic relaxing reagents that enhance the rate of relaxation. The resulting change in the power needed for saturation ($\Delta P_{1/2}$) is a measure of the accessibility of the nitroxide to the solvent containing the relaxation reagent.

When SecA associates with proteoliposomes two solvents are involved, an aqueous phase and a nonpolar phase, thus two collisional reagents are necessary to probe the interactions: the polar complex Ni(II) ethylenediaminediacetate (NiEDDA) for the aqueous environment and O_2 for the hydrophobic lipid phase. The collisional reagents partition between the two phases according to their polarity. Opposite concentration gradients are established normal to the plane of the bilayer: oxygen has its highest concentration at the center of the bilayer, whereas the concentration of NiEDDA is highest at the membrane–aqueous interface and lowest at the center of the bilayer.[21] The difference between the accessibility (given by the parameter, Π) of a spin-labeled residue to polar and nonpolar collisional relaxation reagents is a function of depth. The depth parameter ϕ is defined as $\phi = \ln(\Pi_{O2}/\Pi_{NiEDDA})$ and is a linear function of depth in the hydrophobic phase.[21]

The strategy requires that a series of variants of the protein under study be constructed in which each has a single accessible cysteine that is in the region of interest (see "Materials and methods"). In SecA, cysteine was substituted separately for each aminoacyl residue from 2 through 11 as well as for residues 13, 15, 19, and 20. It should be noted that residue 2 is the first aminoacyl residue present in SecA. The initiating methionine is removed in the cytoplasm. The 14 constructs were modified to introduce a paramagnetic center using the sulfhydryl-specific reagent 1-oxyl-3-(maleimidomethyl)-2,2,5,5-tetramethyl-1-pyrrolidine. Each spin-labeled species is designated by the residue number and amino acid that has been substituted and modified by maleimide chemistry. Thus L2m indicates that leucine at position 2 carries a spin label.

As the first step in the study of depth in the membrane we determined the accessibility parameters (Π) for the spin-labeled residues in the N-terminal region of SecA under conditions in which the SecA was free in solution and also when it was associated with three liposome systems, PLYEG•A,

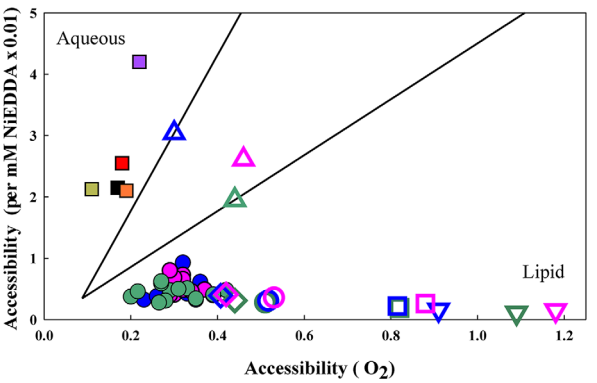

Figure 1. Topographical plot. The color scheme for spin-labeled SecA variants or spin-labeled lipid standards in the three systems is as follows: PLYEG•A, green; PLYEG + A, blue; liposomes + A, pink. Open symbols represent the standards as follows: lipids spin-labeled at head group Δ; in the hydrocarbon chains at C5 ◇, C7 ○, C10 □, C12 ▽. Filled circles, first 10 residues of SecA each with a single spin label at a specific site. Residues that map to the aqueous region are represented as filled squares. Spin-labeled SecA variants free in solution in the absence of liposomes; SecAR13m, black; SecAG11m, orange; SecAF10m, yellow. Spin-labeled SecAF10m free in solution in the presence of neutral PC liposomes, red; spin-labeled SecBT46m free in solution in the presence of *E.coli* liposomes, purple. The lines are drawn to aid the eye in distinguishing the aqueous and the lipid-associated regions.

PLYEG + A and liposomes only. In addition we examined proteins known to be soluble and lipids spin labeled at the polar heads and in the hydrocarbon chains. The data are presented in a topographical plot[22,23] (Fig. 1), which is a phase diagram that distinguishes spin-labeled residues that are in a homogeneous aqueous environment from those that penetrate the bilayer. In this plot the accessibility parameter for NiEDDA (Π_{NiEDDA}) is plotted versus the accessibility parameter for oxygen (Π_{O2}) for each spin-labeled residue. For residues that lay within the bilayer a NiEDDA concentration of 100 m*M* in the aqueous phase is required to achieve a level of the polar reagent within the lipid phase sufficiently high to generate a power saturation curve. On the other hand for a residue exposed to the homogeneous aqueous phase, 100 m*M* NiEDDA results in broadening of the spectral line. Therefore, if line broadening is observed a lower concentration (20 m*M*) is used for power saturation experiments. Thus, in the topographical plot the values for Π_{NiEDDA} are expressed per m*M*. The spread of the data along the Π_{O2} axis reflects the increase in the concentration of O_2 as a function of depth in the bilayer since the collision rate with O_2 determines Π. There are no gradients in the solution phase, thus the spread of data along the axis for Π_{NiEDDA} does not result from differences in concentration of the collisional reagents. Differences in accessibility in a homogenous environment depend on constraints such as very close approaches or contacts between the spin-labeled residues and other atoms in the protein structure that prevent collisions with the paramagnetic reagents.

The data clearly cluster into two areas corresponding to a soluble and a lipid phase. The values for the polar head groups (TEMPO) of lipids incorporated into the three liposome systems (Fig. 1, open triangles) can be taken to indicate the interfacial region between the hydrocarbon phase and the aqueous phase. Lipids carrying spin labels in the fatty acyl chains demonstrate low accessibility to NiEDDA and are distributed along the Π_{O2} axis according to the position of the doxyl label along the length of the hydrocarbon chain (Fig. 1, open symbols, see legend for identity of color and shape). The first 10 aminoacyl residues of SecA when present in the three lipid-containing systems were seen to lie in the lipid phase (filled circles colored according to liposome system, see Fig. 2 for order of residues). In the absence of liposomes the SecA species SecAC98SF10m (yellow square), SecAC98SG11m (orange square), and SecAC98SR13m (black square) were shown to be in the solution phase. Interaction of SecA with membranes requires the presence of anionic lipids; when liposomes comprising only the neutral lipid phosphatidylcholine (PC) were added to SecAC98SF10m, the SecA demonstrated a location in solution (red square). When SecB was spin-labeled at residue T46 and examined in the presence of liposomes, the accessibility indicated a soluble protein (purple square). This is the expected result since SecB has no affinity for lipid.

A plot of the accessibility of the spin-labeled residues of SecA variants in PLYEG•A arranged sequentially reveals a pattern of accessibility to oxygen that is out of phase with the accessibility to NiEDDA [Fig. 2(A)]: when exposure to oxygen is high, accessibility to NiEDDA is low and vice versa. Such a pattern is characteristic of a sequence of aminoacyl resides that is inserted parallel to the plane of the membrane and lies near the interface having some residues exposed to the aqueous phase and others exposed to the hydrocarbon region of the fatty acyl chains. The pattern is most pronounced for residues K4 through G11 in PLYEG•A; however, a similar general pattern was observed for SecA added to PLYEG after reconstitution [Fig. 2(B)] and for SecA associated with empty liposomes [Fig. 2(C)].

Patterns of periodicity in solvent accessibilities of stretches of aminoacyl residues have been used to identify secondary structure.[24] An alternating periodicity of two is characteristic of β structure; whereas, helices display periodicities that reflect the number of residues in a turn. The total number of residues examined here, 10 in a continuous sequence, is not sufficient to fit the data to obtain a

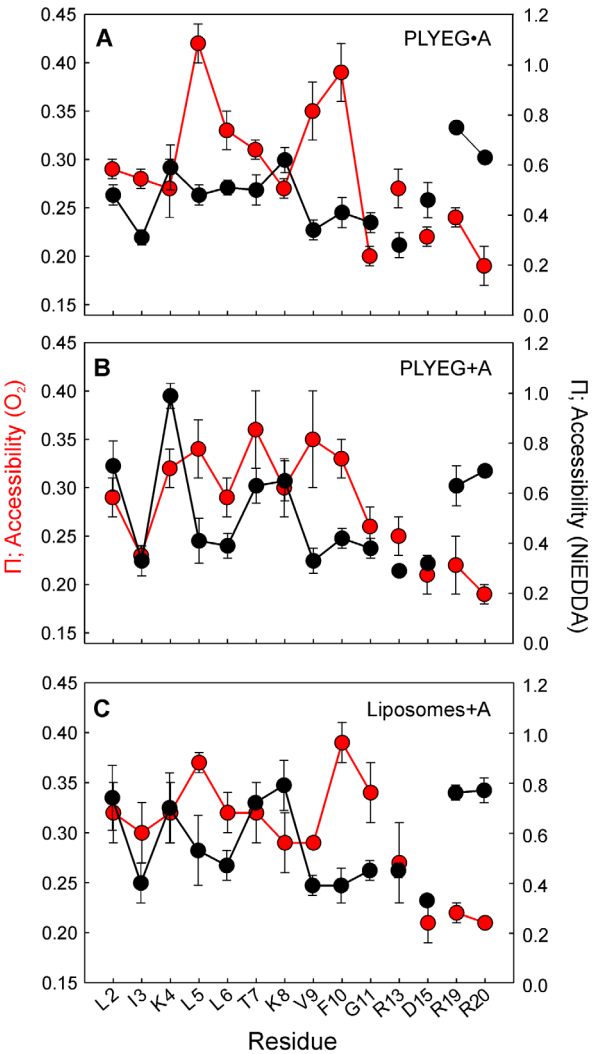

Figure 2. Solvent accessibility of spin-labeled SecA variants. Accessibility to oxygen (red) and NiEDDA (black) for SecA spin-labeled at L2-G11, R13, D15, R19 and R20 in (a) PLYEG•A, (b) PLYEG + A and (c) liposomes + A.

helical periodicity. However, it is clear by visual inspection that in all three systems, the stretches are not in β structure, but rather show weakly helical, loosely coiled patterns. The sequence of residues L2 through G11 forms an amphipathic α helix when displayed in a helical wheel. In the X-ray structure of SecA bound to SecYEG (**PDB 3DIN**) residues 1 through 27 of SecA show α helical structure.[25] In all other structures, the amino-terminal region of SecA is not resolved. This may indicate that the region populates many conformations without having one state more stable than the others. All available X-ray structures were solved in the absence of lipids. We subjected a synthetic peptide mimic of the first 10 aminoacyl residues to analyses by circular dichroism to determine the effect of lipid on the secondary structure. In the absence of lipid the spectrum was typical of a predominantly disordered peptide [Fig. 3(A), black]. In the presence of liposomes the α-helical content of the peptide increased with increasing concentration of lipids, reaching a maximal level of 70% and showed no further increase above 0.75 m*M* lipid. The increase in helical content was at the expense of strands, turns and random coil [Fig. 3(B)]. As described above, the periodicity of the same sequence of amino acids in the intact SecA showed a loose coil but no defined pattern as assessed by accessibility measurements. This is likely the consequence of constraints on the sequence resulting from attachment to the remainder of SecA.

The depth parameter, ϕ, is calculated for each spin-labeled residue from the natural logarithm of the ratio of its accessibility parameters to O_2 and to NiEDDA. The parameter ϕ is related to depth through calibration curves generated using lipids carrying spin labels at known depths. Since the presence of protein in the systems changes the solvent accessibility of the spin-labeled lipids used for calibration (see "Materials and methods" for details), a calibration curve specific for each liposome system must be generated. The calibration curve for depth in PLYEG•A is shown in Figure 4 (cyan squares).

To demonstrate the validity of depth determination using our systems we selected residues that are known to be found in different environments with respect to the membrane (Fig. 4). Firstly, we examined a residue (L20) that is on the surface of a transmembrane helix of Tsr, a chemoreceptor for

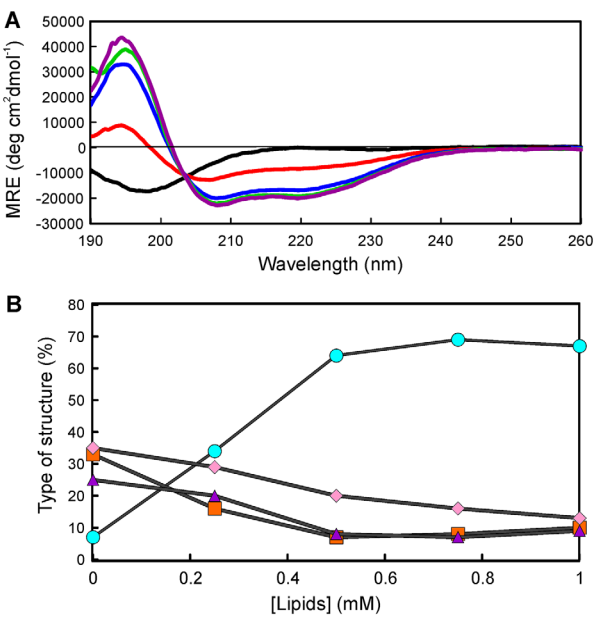

Figure 3. Secondary structure of the peptide mimic of SecAL2 through SecAG11. (a) CD spectra of the synthetic peptide as a function of increasing concentration of liposomes. Lipid concentration 0 mM, black; 0.25 mM, red; 0.5 mM, blue; 0.75 mM, green; 1 mM, purple. (b) Quantification of elements of secondary structure: α helix, cyan; total strand, red; disordered, pink; turns, purple.

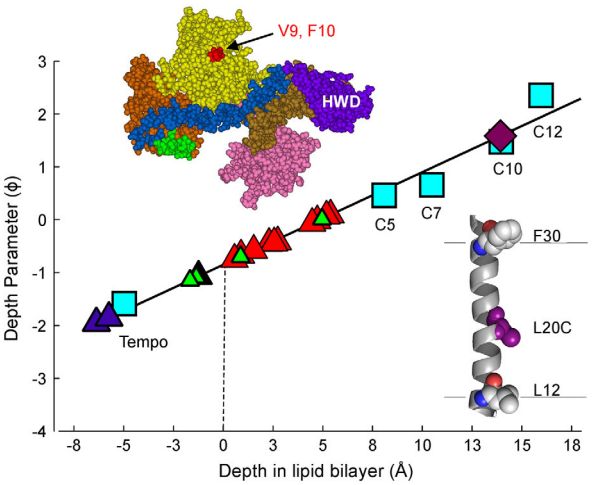

Figure 4. Depth measurements for PLYEG•A. Cyan squares are lipids spin labeled at the positions as indicated. The solid line is a linear fit to these standards. The dotted line through zero corresponds to the position of the phosphate in the polar head group. For spin-labeled residues in SecA the color of the symbols represents a residue located in the domain of the same color (CPK model of SecA, upper left): residues L2 through G11, red triangles; residue C896 in the C-terminal region, black triangle; residues E699 and E729 in the HWD of SecA, dark blue triangles. The purple diamond represents spin-labeled residue L20 in transmembrane Tsr, a transducer of the chemotaxis system in *E.coli*. Lower right: L20 of Tsr shown on a model of the transmembrane helix.[26,27] Upper left: X-ray structure of SecA (**PDB 2FSF** with the PBD modeled in based on *B. subtilis* SecB **PBD 1TF5**, a gift from A. Economou). SecA comprises 901 amino acid residues organized in several domains: two nucleotide binding domains NBD1(yellow) and NBD2 (light brown); preprotein binding domain, PBD, (pink); α-helical scaffold domain, HSD, (blue); α-helical wing domain, HWD, (dark blue); Intramolecular Regulator of ATPase, IRA1, (dark brown); and a short 10-residue α-helix, residues 600–609, (green) that links NBD2 to HSD. The amino-terminal residues 1–8 and the C-terminal domain, residues 836–901, were not resolved in the structure.

serine in *E. coli*. The power saturation results for TsrL20m assembled into proteoliposomes gave a depth of 13.9 Å (purple diamond). This value is within error of the depth (11 Å) calculated from a model of a closely related chemoreceptor for aspartate, Tar.[26,27] Secondly, we tested two residues on SecA, E699m and E729m, in the Helical Wing Domain, that are solvent exposed in an *E.coli* homology model of the SecYEG-SecA X-ray structure[28] (a generous gift from Ian Collinson). When they are assembled into proteoliposomes, PLYEG•A, these residues (Fig. 4, dark blue triangles) were not immersed in the hydrocarbon region; they mapped near the polar head group of the lipids (Tempo, cyan square) as would be expected since SecA is bound to SecY. The C-terminal 70 aminoacyl residues (831–901) of SecA are known to interact with membranes electrostatically.[11] In PLYEG•A SecAC896m (black triangle) was found it to be 2.2 Å below the phosphate head group at the lipid-water interface where electrostatic interactions would occur. The 10 aminoacyl residues located at the N-terminus of SecA variants that had been assembled into PLYEG•A (red triangles) mapped to the hydrocarbon region between the phosphate at the interface and C5 of the fatty acyl chains. The depth of the residues in sequential order is shown in Figure 5.

Comparison of the penetration depths as a function of residue number shows that the residues of the N-terminal region in all three systems lie parallel to the plane of the membrane. Maximal penetration is observed for nonspecific binding of SecA added to empty liposomes (7–8 Å into the bilayer) (Fig. 5). When SecYEG is co-assembled with SecA to give the highly active complexes observed in PLYEG•A, the N-terminal region penetrates the least having the deepest residues at approximately 5 Å. The N-terminal residues of the SecA that was added after the proteoliposomes had been assembled show a pattern of depth that lies between the other two systems. The three most amino-terminal residues, L2, I3, and K4 are at the same depth as in PLYEG•A, and diverge at later positions to follow closely the pattern for the empty liposomes until residue V9. The penetration of G11 in SecYEG•A is the least among the three systems. We extended our analyses beyond the continuous stretch from 2 to 11 to include four charged residues beyond G11, arginines at positions 13, 19, and 20 as well as an aspartate at position 15. It is clear from examination of Figure 5 that as the polypeptide approaches the structural body of SecA, the chain is emerging from the bilayer. The arginines at positions 19 and 20 lie in the polar head region of the bilayer, approximately 2 Å above the phosphate group. Residues 19

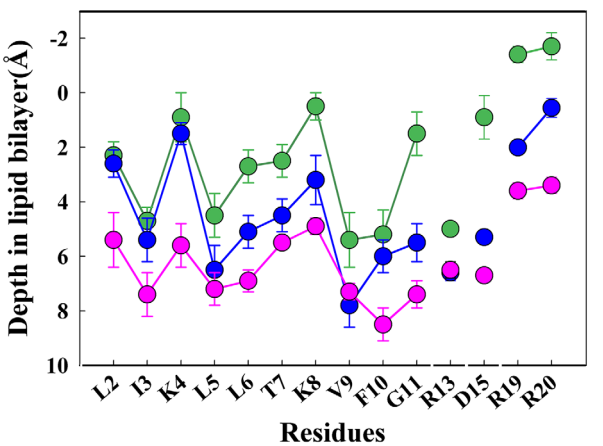

Figure 5. Penetration depth into the bilayer of the N-terminal region. Depth in the bilayer of spin-labeled aminoacyl residues 2–11, 13, 15, 19, and 20 in full length SecA: incorporated into PLYEG (PLYEG•A), green; added to PLYEG (PLYEG + A), blue; added to liposomes (liposomes + A), pink. The phosphate group is taken as zero.

and 20 of SecA in the other two systems remain well inserted into the hydrocarbon region. As seen with the other aminoacyl residues, the charged residues are closest to the interface of the membrane when the SecA is co-assembled with SecYEG, deepest when SecA is added to liposomes and intermediate when added to preformed proteoliposomes SecYEG.

Our previous work using atomic force microscopy to image SecA associated with the three liposome systems offers an explanation for the different depths observed in the three systems. When proteoliposomes were formed by co-assembly, the great majority of SecA was found in one homogeneous population that represents the active translocon and displayed a height of 40 Å, corresponding to SecA bound to SecYEG as observed in the X-ray structure of the complex.[20,25] In contrast, when SecA was added to preformed PLYEG or to empty liposomes, there was a wide distribution of heights with no prominent peak. The amino-terminal region of molecules of SecA that were bound directly to lipids, as can occur with PLYEG + A and with liposomes lacking SecYEG, would be able to penetrate more deeply than it could if SecA were held at a distance from the lipid surface by interaction with SecYEG. The co-assembled PLYEG•A have six times more active units of SecYEG than do the PLYEG to which SecA is added. Thus, PLYEG with SecA added would have a mixed population of SecA, between the extremes of mostly bound to SecYEG as in PLYEG•A and all bound directly to lipids (liposomes + A) thereby accounting for the three different patterns of depth.

Discussion

Both *in vivo* and *in vitro* the interaction of SecA with anionic lipids is crucial for translocation through SecYEG.[29,30] Based on the observation that deletion of 20 aminoacyl residues from the N-terminus of SecA eliminated translocation *in vitro*, but activity could be restored by tethering the truncated SecA via a His-tag to Ni-NTA lipids incorporated into proteoliposomes, Bauer *et al*. proposed that the only function of the deleted residues is to tether SecA to the membrane.[31] In contrast, Koch *et al*. proposed that the association with lipid is an essential intermediate step that induces a change in conformation of SecA to prime it for high affinity binding to SecYEG.[32] The nonspecific interaction of SecA to anionic lipids is mediated both by the amino- and carboxyl-terminal regions of SecA.[31,32] Both of these regions are also involved in interactions that stabilize a complex of two protomers of SecA to a tetramer of SecB that has a precursor bound. This complex is important for directing the precursor to the translocon. The C-terminal 21 amino acids of SecA, which contains zinc, binds a negatively charged patch on the flat β sheets on the sides of SecB.[33] The first 10 aminoacyl residues of SecA bind the C-terminal 14 residues of SecB.[34] In addition, the same N-terminal region of SecA protomers makes interfacial contacts that stabilize the dimeric form of SecA.[34–37]

At many points, as SecA moves through the cycle of export, there is a dynamic exchange of the N-terminal region with its multiple binding partners. Free in the cytoplasm the sequence stabilizes the dimeric form of SecA. Upon interaction with SecB, which carries a precursor, the N-termini of both protomers of SecA would bind to the C-termini of the SecB tetramer resulting in a complex having a stoichiometry of two protomers of SecA to one tetramer of SecB (A2:B4).[34] When the N-termini of SecA associate with SecB, the equilibrium of SecA is shifted toward monomer since the interactions of the N-termini at the dimer interface are disrupted. This is consistent with the finding that SecA does not bind SecB as a dimer, but rather as two protomers on opposite sides of SecB,[38] which has the precursor ligand wrapped around it.[39–41] In subsequent steps along the pathway the precursor must be transferred from SecB to SecA and on to the translocon. The affinity of SecB for precursors is in the range of 50 to several hundred nanomolar[42] whereas that of SecA for precursor is in the micromolar range.[43] Therefore, transfer from SecB to SecA must involve a change of relative affinities. We have proposed previously[34,44–46] that the association and/or dissociation of the multiple sites of interaction between SecA and SecB are likely to be involved in the transfer of precursor. Both the SecA dimer and the SecB tetramer, organized as a dimer of dimers, display twofold symmetry and yet the contacts stabilizing the complex are distributed asymmetrically.[34,47] The C-terminal zinc-containing region of each protomer of SecA binds to the flat, β sheet formed on the side of each dimer of the SecB tetramer. Only one of the protomers of SecA has additional stabilizing contacts as demonstrated by the observation that breaking the contacts between the C-termini of SecA and the sides of SecB releases one protomer of SecA and leaves the other bound in a complex of one protomer of SecA to tetrameric SecB (A1:B4).[34] The contacts stabilizing the A1:B4 complex involve the C-terminal tails of SecB. One tail binds the N-terminal 10 aminoacyl residues of SecA and a second SecB tail binds to SecA at the 10 aminoacyl stretch, residues 600–610, which links NBD2 to the HSD.[38] A model of the source of asymmetry among these contacts within a SecB:SecA complex based on a study of heterotetrameric species of SecB proposes that the N-terminal 10 residues and the residues in the 600 region of one SecA protomer bind tails of SecB protomers that lie directly opposite each other across the dimer interface [for details of the model see Ref. 47]. The dimer interface forms a groove that binds precursors.[39,40] Haiman *et al*.[48] using EPR

spectroscopic techniques showed that the distance between spin labels on opposite dimers at the edge of the binding groove changed when a ligand bound. The binding of a protomer of SecA across the interface might exert a strain resulting in a conformational change to decrease the affinity of precursor for SecB. This would allow transfer of precursor from SecB to SecA within the complex. At the membrane both the N-termini and the C-termini of SecA would bind the bilayer thereby disrupting the SecA:-SecB complex. At that point SecA carrying the precursor would bind the SecYEG translocon for movement of the precursor through the membrane.

The proposed competition between partitioning of the N-terminus of SecA into the membrane and binding to SecB requires that the strength of the two interactions be similar. The ΔG of binding of a peptide mimic of SecA residues L2–G11 to the SecB tail is approximately—6 kcal mol^{-1} as determined by titration calorimetry.[46] Interaction of the same peptide with supported lipid bilayers was studied in a single molecule assay using atomic force spectroscopy.[49] The magnitudes of the forces of association and dissociation of the peptide that partitions into the bilayer were fitted to a theoretical model to determine the energy barrier that was overcome to pull the peptide out. The value obtained was approximately 4 kcal mol^{-1}. Thus it appears that both interactions have similar strengths and a competition between them is feasible.

The X-ray structure of *T. maritima* SecA bound SecYEG[25] shows SecA interacting with only the surface elements of SecY, poised above the lipid bilayer. Recent results of an elegant *in vivo* photocrosslinking study from the laboratory of Donald Oliver[19] are inconsistent with this structure. That *in vivo* work showed that SecA penetrates deeply into the SecY channel to interact with transmembrane helices as well as will periplasmic regions.

In the work presented here we have shown that when SecA is productively associated with SecYEG in proteoliposomes SecYEG•A, the N-terminal 10 aminoacyl residues penetrate the membrane to lie parallel to the plane of the bilayer at a depth of approximately 5 Å. As discussed in Koch *et al*.[32] in order for SecA to simultaneously have the N-terminal region in the lipid bilayer and to bind to the surface of SecY, would require a large conformational change. Based on comparison of SecYEG complexes in nanodiscs containing different ratios of lipid to SecYE, Koch *et al*.[32] established that the initial interaction of SecA with lipids is an important intermediate step in binding SecYEG. They proposed that SecA undergoes a large conformational change activating it for binding productively to SecY. Since the complex in the X-ray structure was crystallized in the presence of detergent, which displaced the lipids, that structure may represent SecA before a conformational change that would allow it to integrate deeply into the channel, as observed by Banerjee *et al*.,[19] and to have the N-terminal region penetrate the bilayer directly as we have reported here. Combining our work on interactions of SecA with its binding partner, SecB, as discussed earlier in the text, and the work presented here, we propose that not only the binding to SecA to lipids induces a conformational change that allows it to bind SecYEG, as proposed by Koch *et al*.,[32] but also that the competition between the N-terminal region of SecA binding to SecB and partitioning into the lipid phase might initiate transfer of precursor from SecB to SecA, facilitating the subsequent movement of precursor through the translocon.

Materials and Methods

Bacterial strains and plasmids

Site-directed spin labeling requires that the only accessible cysteine is the target to be modified. Wild-type SecA includes four native cysteines, three of which bind zinc (Cys885, Cys887, and Cys896) and are not available for labeling. Therefore, only one residue, Cys98 was replaced with serine (SecAC98S) to create the parent of all other variants. All substitutions were made by site-directed mutagenesis (Quick Change, Stratagene). The SecA proteins with single accessible cysteines introduced into 14 residues in the N-terminal region were purified from strains of JM109(DE3), which carry derivatives of the plasmid, pMAN400[50] which carries *secAC98S* under control of the Tac promoter. Site-directed mutagenesis created a series of plasmids encoding variants of SecAC98S, each carrying an introduced cysteine at the position indicated: pAL741, L2C; pAL742, I3C; pAL773, K4C; pAL743, L5C; pAL744, L6C; pAL745, T7C; pAL746, K8C; pAL608, V9C; pAL747, F10C; pAL454, G11C; pAL787, R13C; pAL788, D15C; pAL790, R19C; pAL791, R20C; pAL924, E699C and pAL947, E729C. SecBT46C was constructed for a previous EPR study.[39] Ampicillin was the antibiotic in the growth media for all strains. The genes carried on plasmids were induced by isopropyl β-D-1-thiogalactopyranoside (IPTG).

Protein purification

SecA, SecB, SecBT46C and SecYEG were purified as previously described.[20] The strains used were as follows: for SecA, RR1/pMAN400;[50] for SecB wild type, BL21(DE3) harboring plasmid pJW25[51] and for SecBT46C, strain BL21(DE3) *secB*::*Tn5 srl*::*Tn10 recA* harboring plasmid pAL297;[39] for SecYEG C43(DE3) harboring a plasmid encoding *secE* with a His-tag at the N-terminus, *secYC329S, C385S*, and *secG*.[52]

Purification of all SecA single-cysteine variants were carried out using the following protocol. Cells

were grown in LB media at 35°C with shaking to an optical density (OD) of 0.5 at 560 nm. Zinc sulfate was added to a final concentration of 0.1 m*M* and growth continued for 10 min, at which time IPTG was added to 0.2 m*M* and growth continued for 2.5 h. Cells were harvested, washed and suspended in 20 m*M* Tris–Cl, pH 8.0, 2 m*M* DTT to a final OD of 120 at 560 nm. The cell suspension was frozen by dripping into liquid nitrogen and stored at −70°C until needed. The suspension was rapidly thawed in 20 m*M* Tris–Cl pH 8.0, 1 m*M* phenylmethylsulfonyl fluoride, 2 m*M* DTT, and 0.15 mg/mL lysozyme at a volume equivalent to twice the weight of the frozen cell suspension. Cells were frozen by rapidly dripping into liquid nitrogen and thawed by incubating at 40°C in a water bath. Cycles of freeze and thaw were repeated twice to lyse the cells. This method of lysis is important because if EDTA were added, as is usually done, to allow access of lysozyme to the peptidoglycan, then two native cysteines would become spin labeled because a zinc atom, which protects them, would be removed. After lysis, the suspension was incubated on ice for 20 min with DNase (10 μg/mL) and $Mg(OAC_2)$ (3 m*M*), and subsequently centrifuged at 542,000×*g*, 32 min at 4°C, in a TL100.4 rotor (Beckman). The supernatant was filtered using a Millipore Steriflip (membrane pore size: 0.2 μm) and applied to a 5 mL Hitrap Blue HP affinity column (GE Healthcare, USA) equilibrated in 10 m*M* HEPES–KOH pH 7.6, 0.1*M* NaCl, 2 m*M* DTT. The column was washed with the same buffer, and a gradient from 0.1*M* NaCl, 0% ethylene glycol, to 1.5*M* NaCl, 50% ethylene glycol in the column buffer was applied. All contaminants were eluted within the gradient. SecA eluted in a continuation of a wash with 1.5*M* NaCl, 50% ethylene glycol in column buffer, which contains 2 m*M* DTT to keep the cysteines reduced. Fractions containing SecA were pooled, the pool was concentrated and stored at −80°C.

Final concentrations of SecA and SecB were determined spectrophotometrically using extinction coefficients at 280 nm of 78,900 M^{-1} cm^{-1} for SecA monomer, and 47,600 M^{-1} cm^{-1} for SecB tetramer. The concentrations of SecYEG were determined using quantitative SDS polyacrylamide gel electrophoresis with a standard of pure SecYEG. Concentrations are expressed as tetrameric SecB, monomeric SecA, and monomeric SecYEG unless otherwise indicated.

Spin-labeling of proteins

Variants of protein labeled with 1-oxyl-3-(maleimidomethyl)-2,2,5,5-tetramethyl-1-pyrolidine (Toronto Research Chemicals, ON, Canada) are designated by the amino acid and residue number that has been substituted and modified by the nitroxide through reaction of the cysteine via maleimide chemistry. Thus, K8m indicates lysine at position 8 carries the spin label. Just before spin labeling, reducing agent (DTT) was removed by exchange into 10 m*M* HEPES–KOH, 0.3*M* KOAc, pH 7.0, using a Nap10 column (GE Healthcare, USA). A threefold molar excess of spin labeling reagent over cysteine was added from a stock of 50 m*M* in MeOH, which had been stored in the dark at −80°C. The final MeOH concentration during labeling was kept below 1%. The labeling reaction was carried out in the dark at room temperature for 3 h and then placed on ice in the dark for 1 h 30 min to complete the reaction. A Nap10 column equilibrated in 10 m*M* HEPES-KOH pH 7.6, 0.3*M* KOAc was used to remove free spin. Fractions of 4 drops (∼200 μL) were collected and those fractions which contained spin-labeled SecA were identified by EPR spectroscopy and pooled. To minimize free spin the pooled fractions were washed twice with 10 m*M* HEPES–KOH, 30 m*M* KOAc, 1 m*M* $Mg(OAC_2)$, pH7.6 in an Amicon Ultra-Centrifugal Concentrator (MWCO: 30 K) and concentrated to approximately 300 μ*M*. The spin-labeled proteins were stored at −80°C. A detailed protocol for spin labeling is given in reference.[53] The continuous wave (CW) EPR spectra for spin-labeled aminoacyl residues L2–G11 are shown in Supporting Information (Fig. S4).

Both the cysteine-substituted and the spin-labeled variants of SecA were folded, demonstrated a monomer–dimer equilibrium and were shown to bind SecB. Only two of the spin-labeled proteins, SecAC98SK4m and SecAC98SI3m, had a significant amount of aggregate (17% and 40%). See Supporting Information Materials for details and examples.

Proteoliposomes

Unilamellar liposomes were prepared by extrusion of *E.coli* polar lipids (Avanti) suspended in 10 m*M* HEPES–KOH, 30 m*M* KOAc, 1 m*M* $Mg(OAC_2)$, pH 7.6 using a Lipofast (Avestin, Ontario, Canada) with a membrane of 100 nm pore diameter. The liposomes were swelled for 3 h at room temperature in the presence of dodecyl beta-D-maltoside (DβM) at a ratio of 4.65 m*M* DβM to 5 m*M* lipids. For PLYEG•A, 10 μ*M* SecYEG and 10 μ*M* spin-labeled SecA monomer were assembled into the liposomes simultaneously. For PLYEG, only 10 μ*M* SecYEG was added. The mixture was rotated at room temperature for 1 h. Biobeads SM-2 (BioRad) in 10 mM HEPES at pH 7.6, 30 m*M* KOAc were added to the mixture at a ratio of 1.4:1 (v:v) to remove detergent, and the mixture was rotated again for approximately 1.5 h at room temperature. Biobeads were removed by centrifugation at 2000*g*, 5 min at 9°C in a GH-3.8 rotor (Beckman Coulter, Allegra 6R). The resulting proteoliposomes were collected by centrifugation at 436,000*g*, 20 min at 4°C, in a TL100.1 rotor (Beckman). The pellet was suspended in 10 m*M* HEPES–KOH, 0.3*M* KOAc, 1 m*M* $Mg(OAc_2)$, pH 7.6, centrifuged, and suspended in the same

buffer in a volume to give approximately 0.25 m*M* spin-labeled protein. The proteoliposomes PLYEG•SecA assembled with spin-labeled SecA variants and PLYEG with the spin-labeled SecA added after reconstitution were shown to be active in an *in vitro* translocation system[20] (see Supporting Information Materials).

EPR power saturation

EPR spectroscopy was performed on an X-band Bruker EMX spectrometer with a dielectric EPR resonator (ER4123D-CW-Resonator Bruker). A sample of 4 μL was loaded into a gas-permeable TPX capillary made of a methyl-pentene polymer (Molecular Specialties, WI). Before collecting data, either N_2 or compressed air (20% O_2) was flushed through the capillary for at least 5 min to equilibrate the sample with the gas and to equilibrate to room temperature. For studies using liposomes, a sample of 8 μL was incubated with a final concentration of either 20 or 100 m*M* NiEDDA (as indicated) for 3 h 30 min. The sample was then subjected to four cycles of freezing in liquid nitrogen and thawing so that the NiEDDA concentration would be the same in the aqueous solution on both sides of the lipid bilayer. During collection of the spectra with NiEDDA, N_2 was flushed through capillary to remove O_2.

To determine the central line width (ΔHpp), spectra were collected using an incident microwave power of 3 mW with a 100 kHz field modulation of 1–3 G as appropriate. For each spectral line, 8 scans were recorded through a 100 G field width with a center field of 3474 G. For power saturation, spectra were acquired at microwave powers over the range of 0.1 to 200 mW in 12 steps of equal increments. At each power, 8 scans were recorded at room temperature with a scan width of 40 gauss and a modulation of 1–3G as appropriate. The spectra collected in the presence of N_2, air (20% O_2) and NiEDDA are used to calculate $P_{1/2}$ (N_2), $P_{1/2}$ (O_2), and $P_{1/2}$ (NiEDDA) using the Labview programs written by Christian Altenbach (University of California, LA). The power saturation parameter for each paramagnetic agent ($\Delta P_{1/2}(x)$, where x is O_2 or NiEDDA) was calculated by subtracting the $P_{1/2}$ value in the absence of a paramagnetic agent ($P_{1/2}$ in N_2) as follows: $\Delta P_{1/2}(x) = P_{1/2}(x) - P_{1/2}(N_2)$, where x is O_2 or NiEDDA. The dimensionless accessibility parameter (Π) is obtained by dividing $\Delta P_{1/2}$ by ΔHpp of the center line of the corresponding EPR signal. Variability among resonators is eliminated by normalization to the accessibility of a standard, 2,2-diphenyl-1-picrylhydrazyl (DPPH).

Generation of calibration curves for the depth parameter

The depth parameter ϕ is calculated from the accessibility values as follows: $\phi = \ln [\Pi(O_2)/\Pi(\text{NiEDDA})]$. The parameter allows determination of depth with reference to calibration curves generated using spin-labeled lipids (Avanti Polar Lipids, AL) that have known depths in the bilayer. We used phospho(tempo)choline (16:0, 18:1) carrying TEMPO on the choline head group and a series of phosphatidylcholine lipids (16:0, 18:0) with doxyl groups at the positions C5, C7, C10, and C12 in the C18 hydrocarbon chains. Calibration curves were generated for the three types of liposomes. SecA was added to empty liposomes and to PLYEG because the presence of protein within the bilayer changes the accessibilty parameters. We used five separate preparations of each type of liposome in which only one species of the spin-labeled lipid was present. All prepartions contained a mixture of *E.coli* polar lipids and the spin-labeled lipid at the ratio of 100:1. The Φ values determined for the spin-labeled lipids that were used as standards in the three systems were plotted as a function of the known depths of the five spin-labeled species: Tempo head group, −5 Å;[54] and four doxyl groups on the hydrocarbon chains,[55] C5, 8.1 Å; C7, 10.5 Å; C10, 14 Å; and C12, 16 Å. The phosphate group of the lipid is taken as zero. The calibration curve for PLYEG•A is shown in Figure 4 (cyan squares). For this calibration, power saturation was done four times for TEMPO, eight times for 5-doxyl, six times for both 7-doxyl, and 12-doxyl and three times for 10-doxyl. For liposomes + A and PLYEG + A each data point was done three times. Using the following equations obtained from linear fits to the data, depths in the lipid bilayer for each residue on SecA in the three systems were determined: PLYEG•A, $y = 0.18x - 0.91$; PLYEG + SecA, $y = 0.19x - 1.43$; liposomes + SecA, $y = 0.26x - 2.2$.

Circular dichroism spectroscopy

Spectra were recorded from 190 to 260 nm in a 1 mm path length quartz cuvette at 8°C using a JASCO J-815 spectrophotometer. The step-size was 0.5 nm, the bandwidth, 1 nm and the scan rate, 20 nm/min. Smoothed, background-corrected spectra were fitted using the CDSSTR secondary structure analysis method[56] accessed through the DichroWeb web-interface ENREF_33[57] located at http://dichroweb.cryst.bb.ac.uk. Reference set 4, which is optimized for the spectral region between 190 and 240 nm was used for all spectra. The peptide concentration was 45 μ*M*, and total lipid concentration was varied between 0 and 1 m*M* as given.

Acknowledgements

We thank Angela Lilly for site-directed mutagenesis and construction of most of the plasmids; Chunfeng Mao with the help of Weijiang Ying, from the Department of Chemistry, University of Missouri for the synthesis of NiEDDA. We are grateful to Anthony Sperber for establishing power saturation

in our laboratory, and Jennine M. Crane and Chunfeng Mao for helpful discussions and assistance with the preparation of the manuscript. We thank Priya Bariya and Gavin King for careful readings of the manuscript. We appreciate the generous gift of crystalline DPPH from Wayne Hubbell, Department of Chemistry and Biochemistry, UCLA. This work was supported by an endowment from the Hugo Wurdack Trust at the University of Missouri and National Institutes of Health Grant GM29798 to L.L.R.

References

1. Driessen AJM, Nouwen N (2008) Protein translocation across the bacterial cytoplasmic membrane. Annu Rev Biochem 77:643–666.
2. Randall LL, Hardy SJS (1986) Correlation of competence for export with lack of tertiary structure of the mature species: a study *in vivo* of maltose-binding protein in *E. coli*. Cell 46:921–928.
3. Cabelli RJ, Chen L, Tai PC, Oliver DB (1988) SecA protein is required for secretory protein translocation into *E. coli* membrane vesicles. Cell 55:683–692.
4. Cabelli RJ, Dolan KM, Qian LP, Oliver DB (1991) Characterization of membrane-associated and soluble states of SecA protein from wild-type and SecA51(TS) mutant strains of *Escherichia coli*. J Biol Chem 266: 24420–24427.
5. Chen X, Xu H, Tai PC (1996) A significant fraction of functional SecA is permanently embedded in the membrane. SecA cycling on and off the membrane is not essential during protein translocation. J Biol Chem 271:29698–29706.
6. Chen X, Brown T, Tai PC (1998) Identification and characterization of protease-resistant SecA fragments: SecA has two membrane-integral forms. J Bacteriol 180:527–537.
7. Hartl FU, Lecker S, Schiebel E, Hendrick JP, Wickner W (1990) The binding cascade of SecB to SecA to SecY/E mediates preprotein targeting to the *E. coli* plasma membrane. Cell 63:269–279.
8. Douville K, Price A, Eichler J, Economou A, Wickner W (1995) SecYEG and SecA are the stoichiometric components of preprotein translocase. J Biol Chem 270: 20106–20111.
9. Matsumoto G, Yoshihisa T, Ito K (1997) SecY and SecA interact to allow SecA insertion and protein translocation across the *Escherichia coli* plasma membrane. EMBO J 16:6384–6393.
10. Breukink E, Keller RCA, Kruijff BD (1993) Nucleotide and negatively charged lipid-dependent vesicle aggregation caused by SecA: evidence that SecA contains two lipid-binding sites. FEBS Lett 331:19–24.
11. Breukink E, Nouwen N, van Raalte A, Mizushima S, Tommassen J, de Kruijff B (1995) The C terminus of SecA is involved in both lipid binding and SecB binding. J Biol Chem 270:7902–7907.
12. Keller RC (2011) The prediction of novel multiple lipid-binding regions in protein translocation motor proteins: a possible general feature. Cell Mol Biol Lett 16:40–54.
13. Breukink E, Demel RA, De Korte-Kool G, De Kruijff B (1992) SecA insertion into phospholipids is stimulated by negatively charged lipids and inhibited by ATP: a monolayer study. Biochemistry 31:1119–1124.
14. Ulbrandt ND, London E, Oliver DB (1992) Deep penetration of a portion of *Escherichia coli* SecA protein into model membranes is promoted by anionic phospholipids and by partial unfolding. J Biol Chem 267: 15184–15192.
15. Ahn T, Kim H (1994) SecA of *Escherichia coli* traverses lipid bilayer of phospholipid vesicles. Biochem Biophys Res Commun 203:326–330.
16. Keller RCA, Snel MME, De Kruijff B, Marsh D (1995) SecA restricts, in a nucleotide-dependent manner, acyl chain mobility up to the center of a phospholipid bilayer. FEBS Lett 358:251–254.
17. Wang HW, Chen Y, Yang H, Chen X, Duan MX, Tai PC, Sui SF (2003) Ring-like pore structures of SecA: implication for bacterial protein- conducting channels. Proc Natl Acad Sci USA 100:4221–4226.
18. Hsieh Y-h, Zhang H, Lin B-r, Cui N, Na B, Yang H, Jiang C, Sui S-f, Tai PC (2011) SecA alone can promote protein translocation and ion channel activity: SecYEG Increases efficiency and signal peptide specificity. J Biol Chem 286:44702–44709.
19. Banerjee T, Zheng Z, Abolafia J, Harper S, Oliver D (2017) The SecA protein deeply penetrates into the SecYEG channel during insertion, contacting most channel transmembrane helices and periplasmic regions. J Biol Chem 292:19693–19707.
20. Mao C, Cheadle CE, Hardy SJS, Lilly AA, Suo Y, Gari RRS, King GM, Randall LL (2013) Stoichiometry of SecYEG in the active translocase of *Escherichia coli* varies with precursor species. Proc Natl Acad Sci USA 110:11815–11820.
21. Altenbach C, Greenhalgh DA, Khorana HG, Hubbell WL (1994) A collision gradient method to determine the immersion depth of nitroxides in lipid bilayers: application to spin-labeled mutants of bacteriorhodopsin. Proc Natl Acad Sci USA 91:1667–1671.
22. Hubbell WL, Altenbach C (1994) Investigation of structure and dynamics in membrane proteins using site-directed spin labeling. Curr Opin Struct Biol 4:566–573.
23. Frazier AA, Wisner MA, Malmberg NJ, Victor KG, Fanucci GE, Nalefski EA, Falke JJ, Cafiso DS (2002) Membrane orientation and position of the C2 domain from cPLA2 by site-directed spin labeling. Biochemistry 41:6282–6292.
24. Klug CS, Feix JB (2008) Methods and applications of site-directed spin labeling EPR spectroscopy. Methods Cell Biol 84:617–658.
25. Zimmer J, Nam Y, Rapoport TA (2008) Structure of a complex of the ATPase SecA and the protein-translocation channel. Nature 455:936–943.
26. Peach ML, Hazelbauer GL, Lybrand TP (2002) Modeling the transmembrane domain of bacterial chemoreceptors. Protein Sci 11:912–923.
27. Boldog T, Hazelbauer GL (2004) Accessibility of introduced cysteines in chemoreceptor transmembrane helices reveals boundaries interior to bracketing charged residues. Protein Sci 13:1466–1475.
28. Bostina M, Mohsin B, Kuhlbrandt W, Collinson I (2005) Atomic model of the *E. coli* membrane-bound protein translocation complex SecYEG. J Mol Biol 352: 1035–1043.
29. de Vrije T, de Swart RL, Dowhan W, Tommassen J, de Kruijff B (1988) Phosphatidylglycerol is involved in protein translocation across *Escherichia coli* inner membranes. Nature 334:173–175.
30. Kusters R, Dowhan W, de Kruijff B (1991) Negatively charged phospholipids restore prePhoE translocation across phosphatidylglycerol-depleted *Escherichia coli* inner membranes. J Biol Chem 266:8659–8662.

31. Bauer BW, Shemesh T, Chen Y, Rapoport TA (2014) A "push and slide" mechanism allows sequence-insensitive translocation of secretory proteins by the SecA ATPase. Cell 157:1416–1429.
32. Koch S, de Wit JG, Vos I, Birkner JP, Gordiichuk P, Herrmann A, van Oijen AM, Driessen AJM (2016) Lipids activate SecA for high affinity binding to the SecYEG complex. J Biol Chem 291:22534–22543.
33. Zhou J, Xu Z (2003) Structural determinants of SecB recognition by SecA in bacterial protein translocation. Nat Struct Biol 10:942–947.
34. Randall LL, Crane JM, Lilly AA, Liu G, Mao C, Patel CN, Hardy SJ (2005) Asymmetric binding between SecA and SecB two symmetric proteins: implications for function in export. J Mol Biol 348:479–489.
35. Hunt JF, Weinkauf S, Henry L, Fak JJ, McNicholas P, Oliver DB, Deisenhofer J (2002) Nucleotide control of interdomain interactions in the conformational reaction cycle of SecA. Science 297:2018–2026.
36. Jilaveanu LB, Zito CR, Oliver D (2005) Dimeric SecA is essential for protein translocation. Proc Natl Acad Sci USA 102:7511–7516.
37. Vassylyev DG, Mori H, Vassylyeva MN, Tsukazaki T, Kimura Y, Tahirov TH, Ito K (2006) Crystal structure of the translocation ATPase SecA from *Thermus thermophilus* reveals a parallel, head-to-head dimer. J Mol Biol 364:248–258.
38. Suo Y, Hardy SJS, Randall LL (2011) Orientation of SecA and SecB in complex, derived from disulfide cross-linking. J Bacteriol 193:190–196.
39. Crane JM, Suo Y, Lilly AA, Mao C, Hubbell WL, Randall LL (2006) Sites of interaction of a precursor polypeptide on the export chaperone SecB mapped by site-directed spin labeling. J Mol Biol 363:63–74.
40. Lilly AA, Crane JM, Randall LL (2009) Export chaperone SecB uses one surface of interaction for diverse unfolded polypeptide ligands. Protein Sci 18:1860–1868.
41. Huang C, Rossi P, Saio T, Kalodimos CG (2016) Structural basis for the antifolding activity of a molecular chaperone. Nature 537:202–206.
42. Randall LL, Topping TB, Suciu D, Hardy SJS (1998) Calorimetric analyses of the interaction between SecB and its ligands. Protein Sci 7:1195–1200.
43. Gouridis G, Karamanou S, Gelis I, Kalodimos CG, Economou A (2009) Signal peptides are allosteric activators of the protein translocase. Nature 462:363–367.
44. Randall LL, Crane JM, Liu G, Hardy SJS (2004) Sites of interaction between SecA and the chaperone SecB, two proteins involved in export. Protein Sci 13:1124–1133.
45. Patel CN, Smith VF, Randall LL (2006) Characterization of three areas of interactions stabilizing complexes between SecA and SecB, two proteins involved in protein export. Protein Sci 15:1379–1386.
46. Randall LL, Henzl MT (2010) Direct identification of the site of binding on the chaperone SecB for the amino terminus of the translocon motor SecA. Protein Sci 19:1173–1179.
47. Suo Y, Hardy SJS, Randall LL (2015) The basis of asymmetry in the SecA:SecB complex. J Mol Biol 427:887–900.
48. Haimann MM, Akdogan Y, Philipp R, Varadarajan R, Hinderberger D, Trommer WE (2011) Conformational changes of the chaperone SecB upon binding to a model substrate–bovine pancreatic trypsin inhibitor (BPTI). Biol Chem 392:849.
49. Matin TR, Sigdel KP, Utjesanovic M, Marsh BP, Gallazzi F, Smith VF, Kosztin I, King GM (2017) Single-molecule peptide-lipid affinity assay reveals interplay between solution structure and partitioning. Langmuir 33:4057–4065.
50. Kawasaki H, Matsuyama S, Sasaki S, Akita M, Mizushima S (1989) SecA protein is directly involved in protein secretion in *Escherichia coli*. FEBS Lett 242:431–434.
51. Weiss JB, Ray PH, Bassford PJ Jr. (1988) Purified SecB protein of *Escherichia coli* retards folding and promotes membrane translocation of the maltose-binding protein *in vitro*. Proc Natl Acad Sci USA 85:8978–8982.
52. Collinson I, Breyton C, Duong F, Tziatzios C, Schubert D, Or E, Rapoport T, Kuhlbrandt W (2001) Projection structure and oligomeric properties of a bacterial core protein translocase. EMBO J 20:2462–2471.
53. Oh KJ, Altenbach C, Collier RJ, Hubbell WL (2000) Site-directed spin labeling of proteins. Applications to diphtheria toxin. Methods Mol Biol 145:147–169.
54. Farahbakhsh ZT, Altenbach C, Hubbell WL (1992) Spin labeled cysteines as sensors for protein-lipid interaction and conformation in rhodopsin. Photochem Photobiol 56:1019–1033.
55. Dalton LA, McIntyre JO, Fleischer S (1987) Distance estimate of the active center of d-beta-hydroxybutyrate dehydrogenase from the membrane surface. Biochemistry 26:2117–2130.
56. Sreerama N, Woody RW (2000) Estimation of protein secondary structure from circular dichroism spectra: comparison of CONTIN, SELCON, and CDSSTR methods with an expanded reference set. Anal Biochem 287:252–260.
57. Whitmore L, Wallace BA (2008) Protein secondary structure analyses from circular dichroism spectroscopy: methods and reference databases. Biopolymers 89:392–400.